Pure & Appl. Chem., Vol. 61, No. 2, pp. 143–152, 1989.
Printed in Great Britain.

Phase behavior in fluid and solid mixtures at high pressures

William B. Streett

School of Chemical Engineering, Cornell University, Ithaca, NY 14850, USA

Abstract - Following the description of a classification scheme for fluid phase diagrams in two-component systems, based on boundary lines in pressure-temperature space, the three-dimensional features of several important classes of pressure-temperature-composition (PTX) phase diagrams for two-component mixtures at high pressures (up to 100 kbar) are described. The discussion includes two-and three-phase equilibria between gas, liquid and solid phases, with emphasis on the qualitative effects of pressure on these systems and the picture of continuity between different types of critical and three-phase phenomena that has emerged from studies at high pressures.

INTRODUCTION

The variety and complexity of phase behavior observed in early experiments, even in two-component systems of relatively simple molecules, seemed, at first, chaotic. The discovery of the phase rule by Gibbs in 1875 brought a measure of order by providing a framework for the interpretation and classification of phase diagrams, and led to a period of intense experimental study, lasting until about 1915. During this period most of the known types of fluid phase diagrams were discovered; however, much of this knowledge gradually disappeared from the literature of physics and chemistry. A revival of interest occurred in the second quarter of this century, sparked by the growth of chemical engineering technology, especially in the natural gas and petroleum industries, and many properties of multi-component phase diagrams were rediscovered and further explored by chemical engineers. Concurrently, the development of high pressure techniques led to systematic studies, by physicists and engineers, of the effects of pressure on phase equilibria in pure substances and mixtures. The study of pressure effects, especially on critical behavior and three-phase separations in binary mixtures, has brought new insights into the relationships between the three types of two-phase equilibria--liquid-liquid, gas-liquid, and gas-gas--that occur in fluid systems. Experiments of the last several decades, especially those of G. M. Schneider, have shown that there are continuous transitions between these three types (ref. 1-3 and other references therein). Streett and co-workers (ref. 4-7) began to explore the effects of pressure on the equilibria between solid and fluid phases, reaching pressures of 10 kbar, and more recently the elegant experiments of Schouten and his colleagues (ref. 8-10) have extended the pressure range to 100 kbar through the use of diamond anvil cells. A picture of the unity and continuity of critical and three-phase phenomena in binary fluid mixtures has emerged, bringing a greater order to the classification and interpretation of many types of phase behavior that previously seemed unrelated, and gas-gas phase separations in highly supercritical fluid mixtures have been observed at pressures up to 100 kbar. More recently the equilibrium between solid and fluid phases at high pressures has been studied in several two-component systems.

PHASE DIAGRAMS FOR TWO-COMPONENT SYSTEMS

In experimental studies of phase diagrams the properties most commonly measured are pressure, temperature and composition (P, T, X) a combination of two field variables, P and T, each of which has the same value in all coexisting phases at equilibrium, and one generalized density variable, X, that in general has different values. From the phase rule it follows that a two-component system can be completely described by a three-dimensional diagram, and here we use PTX diagrams for this purpose. In these diagrams a homogeneous single phase is occupies a volume in PTX space, and the conditions of two-, three- and four-phase equilibrium give rise to pairs of surfaces, triplets of lines and quadruplets of points, respectively. An important geometrical constraint imposed by the use of two field variables requires that these surfaces, lines and points have common projections on the PT plane. Each pair of surfaces representing two coexisting phases projects as a single surface, each triplet of lines representing three coexisting phases projects as a single line, and each quadruplet

of points representing four coexisting phases projects as a single point on the PT plane. A more detailed discussion of geometrical constraints imposed by the phase rule and by the use of field variables has been given by Streett (ref. 7).

The simplest type of PTX diagram for a fluid system is one that describes the gas-liquid equilibrium of a system in which the two components are miscible in all proportions in the liquid phase as well as in the gas phase. An example is shown in Fig. 1(a). Lines $A_\alpha C_\alpha$ and $A_\beta C_\beta$ are the vapor pressure curves of the two components, α and β, in the two PT planes of the diagram, ending in critical points C_α and C_β. The mixture critical line $C_\alpha C_\beta$ is continuous in PTX space. The two surfaces representing coexisting gas and liquid phases in the mixture extend across the diagram and are bounded by the lines $A_\alpha C_\alpha$, $A_\beta C_\beta$ and $C_\alpha C_\beta$. With the P axis vertical, the lower surface represents the gas phase and the upper surface the liquid phase. These shapes of these surfaces are not easily illustrated by shading, because one would be obscured by the other. ***The convention used in Fig. 1, and in Figs. 3, 6-9, is to use sections cut by planes of constant P, T and X--isobars, isotherms and isopleths--and to shade portions of these sections lying within the two-phase region.*** The boundary lines of these planar sections lie in the surfaces representing two coexisting phases--the surfaces of principal interest. Boundary lines of the P-, T- and X-sections lying within the surface representing the liquid phase are shown solid and those lying with the surface representing the gas phase are shown as short-dashed lines. Critical lines are shown as long-dashed lines and three-phase lines as dash-dot lines. Fig. 1(b) shows projections of the boundary lines of the two-phase region on a PT plane, with vertical and horizontal lines to mark the isotherms and isobars shown as shaded sections in Fig. 1(a) (T_1-T_5 and P_1-P_4). Figs. 1(c) and (d) show projections of selected isotherms and isobars on PX and TX planes. A horizontal line through one of the isotherms in Fig. 1(c)--such as d-e-f--is a tie line, a line connecting points that represent coexisting gas and liquid phases at fixed P and T.

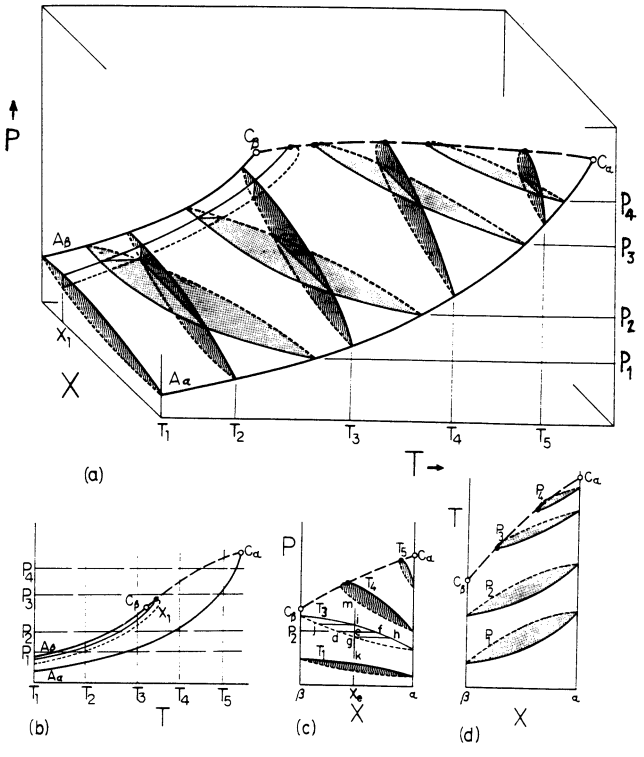

Fig. 1. PTX phase diagram for a two-component system in which the liquids are miscible in all proportions.

CLASSIFICATION AND DESCRIPTION OF HIGH-PRESSURE PHASE DIAGRAMS

Recent experimental and theoretical studies have shown that there are continuous transitions between phase diagrams that exhibit gas-liquid, liquid-liquid and gas-gas phase separations. The most important experimental contribution in this field is the work of G. M. Schneider (ref. 1-3 and other references therein). The two features of his work that are particularly important are: (1) the systematic application of high pressures (up to 7,000 bar) to the study of critical phenomena in mixtures, and (2) the study of families of two-component systems in which one component remains

the same and the other is changed in a systematic way (e.g., CO_2 mixed with families of hydrocarbons of increasing molecular weight). In most of his experiments Schneider concentrated on measurements of the PT traces of critical lines and three-phase lines of the type liquid-liquid-gas. These lines, together with pure-component vapor pressure curves (and azeotropic lines where these occur) form the principal boundaries in PT space of the surfaces representing equilibrium between two fluid phases. Other recent experiments by Streett and co-workers (ref. 4-7) on binary mixtures in which hydrogen, helium or neon is the lighter component have explored critical phenomena, gas-gas phase separations, and the equilibrium between solid and fluid phases at pressures up to 10 kbar. In these systems critical lines and three-phase lines of the type solid-liquid-gas have been measured, and these types of boundary lines have been followed up to 100 kbar in several systems by Schouten and others (ref. 8-10).

In the classification of phase diagrams an important analytical contribution is that of Scott and Van Konynenberg (ref. 11, 12) who demonstrated that most of the experimentally observed binary fluid phase diagrams can be described qualitatively by the van der Waals equation of state applied to mixtures. Using as a basis the PT projections of critical and three-phase lines resulting from their calculations, these authors grouped fluid phase diagrams into five major classes, designated I to IV, and they recognized a sixth class that occurs in several known systems but is not predicted by the van der Waals equation. The classification scheme is outlined in Fig. 2, which illustrates the principal lines (one degree of freedom) and points (zero degrees of freedom) that form boundaries in PT space of the pairs of surfaces that represent equilibrium between two phases. The four types of boundary lines are: (1) pure component vapor pressure curves (solid lines); (2) critical lines (dashed lines); (3) three-phase lines (dash-dot lines); and (4) azeotropic lines (dash-dot-dot lines). The two important types of limiting points are: (1) pure component critical points (circles); and (2) critical end points (triangles) formed by the intersection of a three phase region liquid-liquid-gas

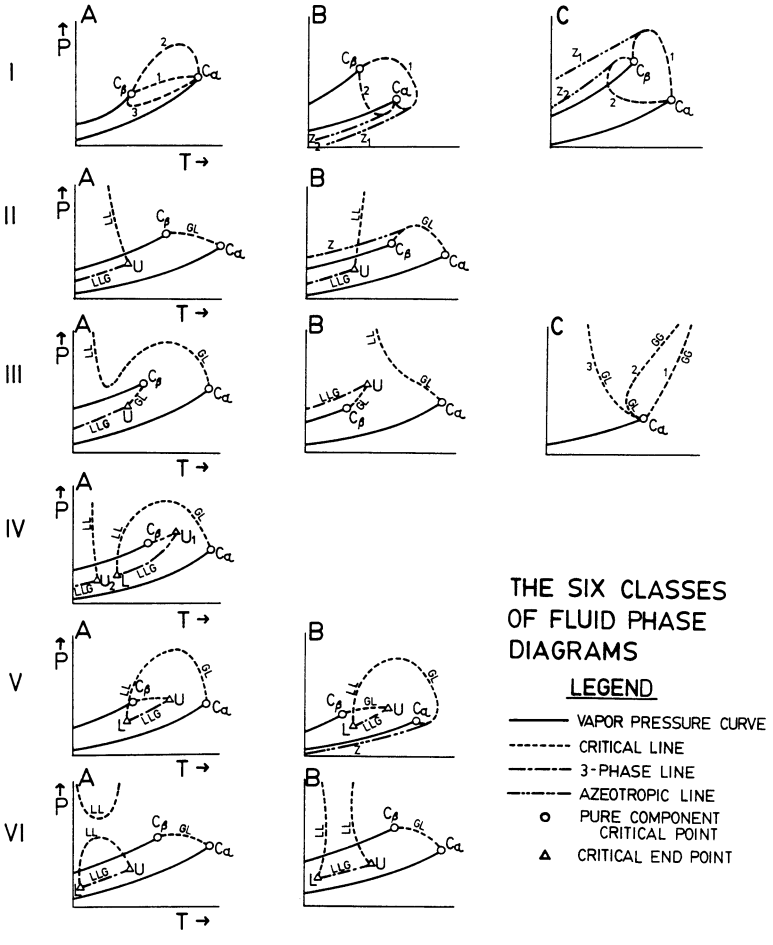

Fig. 2. The six classes of fluid phase diagrams, following the classification scheme of Van Konynenberg and Scott (ref. 11, 12).

with a critical line. A critical end point is a limiting point at which two of three coexisting phases become identical, and they are classed as upper (U) if they represent the maximum temperature at which a three-phase region exists, or lower (L) if the minimum temperature. In Fig. 2, GL indicates gas-liquid, LL liquid-liquid, LLG liquid-liquid-gas, GG gas-gas, and Z an azeotropic line. The lines and points in Fig. 2 provide only skeletal outlines of the phase diagrams. A more complete description requires the use of three-dimensional PTX diagrams. Several examples are considered in the remainder of this paper. The diagrams illustrated are purely qualitative, and do not represent specific real systems. Schneider (ref. 2, 3) has described diagrams for many real systems.

The distinctions between classes of phase diagrams in the classification scheme of Van Konynenberg and Scott are drawn mainly on the basis of critical lines; however, in Fig. 2 several sub-classes (A, B, C) and sub-sub classes (numbered 1, 2, 3) are shown to illustrate the remarkable variety of critical, azeotropic and three-phase lines found in nature. The collection shown here is by no means complete.

In classes I, II and VI the gas-liquid critical line (GL) is continuous between the critical points of the pure components C_α and C_β. In class I the pure liquids are miscible in all proportions (Fig. 1 is of this class) and the critical line can have maxima and minima in pressure and/or temperature. The sub-classes I_B and I_C have azeotropes that occur at maximum temperatures (minimum pressures) and minimum temperatures (maximum pressures), respectively.

In class II there is a liquid-liquid critical line (LL) bounded at low pressures by an upper critical end point (U) where it intersects the three-phase region liquid-liquid-gas (LLG). Class II_B includes an azeotrope (see Fig. 3).

In class VI (which is not predicted by the van der Waals equation but is known from experiments) one or two liquid-liquid critical lines are bounded at low pressures by upper and lower critical end points. In class VI_A there is a gap of complete miscibility between two distinct regions of liquid-liquid phase separation, and in some cases the upper region is absent, or perhaps unobserved because it lies at pressures beyond the range of experiments.

In classes IV and V the branch of the gas-liquid critical line originating in C_α has a maximum in pressure and passes continuously to a liquid-liquid critical line, terminating in a lower critical end point L, and the other branch of the gas-liquid critical line, originating in C_β, ends in an upper critical end point U. In Class IV there is a second liquid-liquid phase separation at lower temperatures, with a liquid-liquid critical line ending in a second upper critical end point U_2.

In the remaining class, III, the branch of the gas-liquid critical line originating in C_α rises to very high pressures, sometimes after passing through maxima and minima in pressure and/or a minimum in temperature. It is this class, and especially the sub-class III_C, that is of principal interest in studies of fluid phase behavior at high pressures. Where the critical lines--and hence phase separations--exist at temperatures above the critical temperatures of the pure components, the separation into two phases is referred to as a gas-gas equilibrium (GG). Schouten (ref. 8-10) has shown that gas-gas phase separations in systems of class III persist to pressures of 100 kbar and higher. This is discussed further below, in the description of Fig. 8.

In interpreting fluid phase diagrams it is useful to keep in mind geometrical constraints on the shape of the PTX surface in the vicinity of critical lines. A critical point is defined as a limiting point at which the differences in properties between two coexisting phases vanish. In isothermal and isobaric sections, as in Figs. 1(c) and (d), lines connecting two coexisting phases (tie lines) are parallel to the X-axis, and it follows that critical points on isotherms and isobars are either maxima or minima, where the PX or TX loop is tangent to a line parallel to the X-axis. This geometric constraint results from the use of two field variables (P and T) as coordinates in the phase diagram. It establishes the additional constraint that in the PT projection the critical line is an *envelope*, tangent to all sections cut by planes of constant composition [Fig 1(b)]. Maxima in P and T in these sections (isopleths) have no particular significance. These geometric constraints can also be deduced from the condition of material stability and the laws of thermodynamics (ref. 13).

Fig. 3 illustrates a system of class II_B in Fig. 2, a system with a liquid-liquid-gas phase separation bounded by an upper critical end point, a continuous gas-liquid critical line, and a minimum-temperature azeotrope. The three-phase region $L_\alpha L_\beta G$ is shaded by parallel lines (It is a "ruled surface" formed by moving a line through space always keeping it perpendicular to the PT plane. This geometric constraint is imposed by the phase rule and by the choice of two field variables, P and T, that are the same in all phases at equilibrium.) The three lines L_α, L_β and G in Fig. 3(a) project as a single line LLG in Fig. 3(b). The isotherm T_2 is at the temperature of the critical end point U, and as a consequence U is a horizontal inflection point on the liquid boundary of T_2, as

shown in Fig. 3(c). The isobar P_1, projected on the TX plane in Fig. 3(d), has two branches, an upper branch in the gas-liquid region and a lower branch in the liquid-liquid region. The systems neon/hydrogen and neon/deuterium exhibit this behavior (ref. 14).

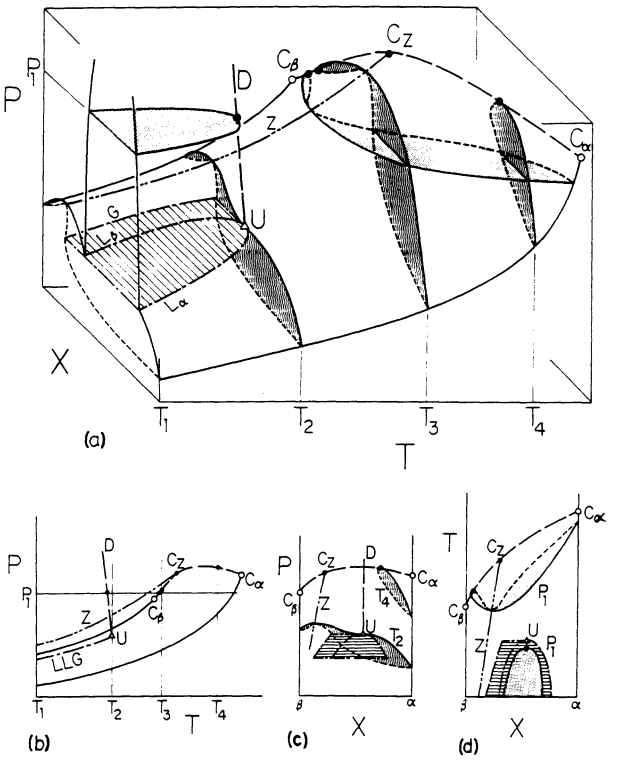

Fig. 3. A system of class II_B in Fig. 2, with a liquid-liquid phase separation and a minimum-temperature azeotrope. Mixtures of neon with hydrogen and deuterium are examples of this type of behavior (ref. 14).

PHASE DIAGRAMS FOR BINARY MIXTURES WITH WIDELY SEPARATED CRITICAL TEMPERATURES

The binary phase diagrams that have been studied at pressures of several kbar or higher fall mainly into the sub-class III_C of Fig. 2, in which the critical temperature of component β lies well below the triple point of component α. The transition from a simple class I_{A1} system to class III is illustrated by the sequence of changes shown in Fig. 4. Fig. 4(a) is a PT projection of the principal boundary lines of a system in which two completely miscible liquids freeze to form partially miscible solid phases S_α and S_β. (Here the level of complexity has been increased by including solid

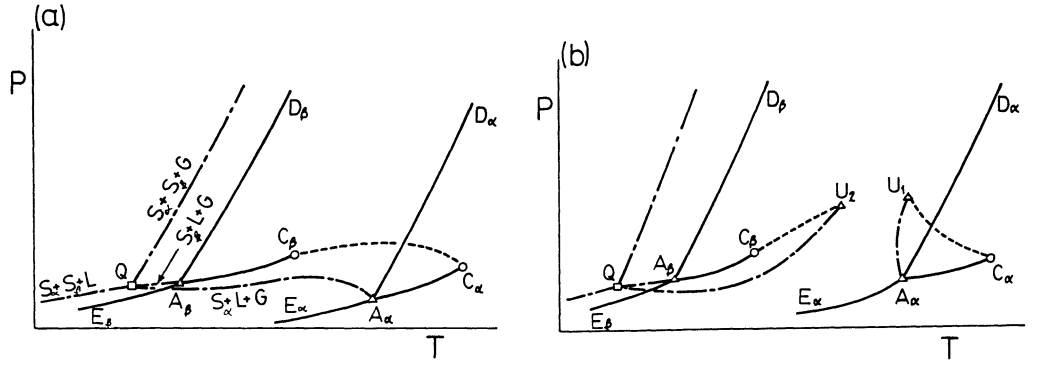

Fig. 4. Transition from class I system, Fig. (a), to class III system, Fig. (b), as the difference between critical temperatures of the pure components increases.

phases, which are not dealt with in the fluid-phase classification scheme of Fig. 2.) The full lines, EA, AD and AC are the sublimation, melting and vapor pressure curves, respectively, of the pure components, α and β. Point Q is a quadruple point, where four phases, S_α, S_β, L and G, are in equilibrium (it consists of four points in PTX space, having a common projection on the PT plane). Radiating from this point are four lines (in PTX space four triplets of lines) representing equilibria between the four possible combinations of three phases drawn from this group. If the temperature of C_β lies far below that of A_α (the triple point of component α) the three-phase region S_α+L+G--line QA_α in Fig. 4(a)--curves upward, and intersects the gas-liquid critical line to form critical end points U_1 and U_2, as shown in Fig. 4(b). No liquid phase exists in the temperature range between U_1 and U_2, where component α is a solid, and component β a supercritical gas, in the pure state. The three-sided region $A_\alpha C_\alpha U_1$, bounded by the vapor pressure curve $A_\alpha C_\alpha$, the critical line $C_\alpha U_1$, and the three-phase boundary $A_\alpha U_1$, is a region of gas-liquid phase separation, bounded on the high pressure side by U_1, at which the gas and liquid phases in equilibrium with a solid phase (S_α) become identical. At temperatures between this three-phase region and U_2, the solid phase of component α is in equilibrium with a β-rich gas phase. If the vapor pressure of α is small at the temperature of C_β and below, which is often the case, the solubility of the α solid phase in the β liquid phase may be vanishingly small, with the result that points Q and U_2 are virtually coincident with A_β and C_β, respectively. In these cases only the right-hand portion of the phase diagram of Fig. 4(b) is of interest for studying phase separations.

With increasing difference between the critical temperatures of the pure components, critical lines and three-phase lines can be arranged in the general sequence shown in Figs. 5(a) to (e). These diagrams are a subset of class III_C of Fig. 2, and the regions of three-phase equilibrium are of the type solid-liquid-gas (SLG). In Fig. 5(a) the SLG three-phase boundary AU has a minimum in temperature and regions of both positive and negative slope, which gives rise to unusual pressure effects on freezing and melting (ref. 23, 25). In Fig. 5(c) the critical line has a temperature minimum and intersects the three-phase line at the critical end point U at temperatures above that of the pure-component critical point C. An example of this behavior is the system helium/argon, where the end point U lies at about 11 kbar and 205 K, about 55 K above the argon critical temperature (ref. 15). If Figs. 5(d) and (e) the critical and three-phase lines do not intersect, and the region of equilibrium between two fluid phases is opened up to very high temperatures at high pressures, and it is these supercritical regions of fluid phase separation that are called gas-gas equilibrium. This term is perhaps misleading, because these phase separations occur in fluid mixtures that have been compressed to liquid-like densities at supercritical temperatures (above the critical temperatures of the pure components).

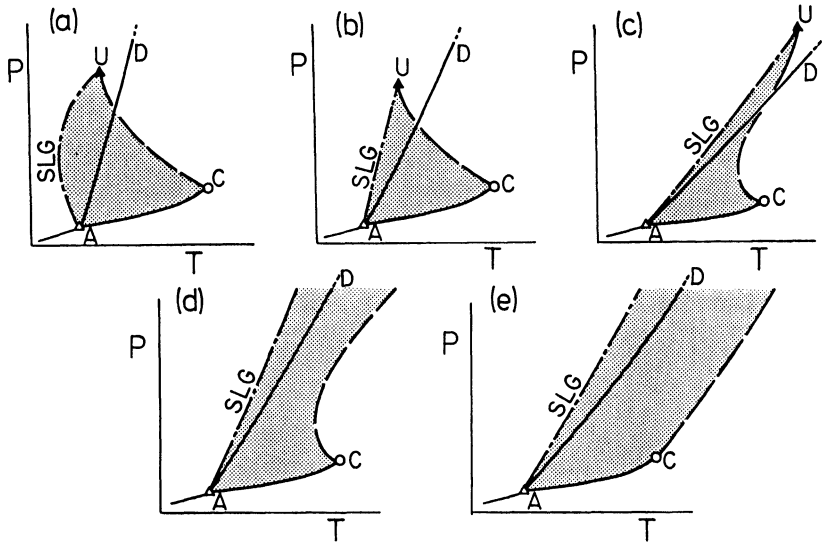

Fig. 5. Sequence of changes in critical lines and solid-liquid-gas three-phase lines as the difference in pure-component critical temperatures increases. PTX diagrams corresponding to Figs. (b) and (d) are shown in Figs. 7 and 8, respectively.

The work of Schneider (ref. 1-3) clearly shows that there is a logical continuity between phase diagrams that exhibit gas-gas equilibria and those characterized by more familiar gas-liquid and liquid-liquid behavior. The evidence suggests that gas-gas phase separations can best be described as liquid-liquid phase separations displaced to high temperatures at high pressures. These separations occur in mixtures that would very likely form partially miscible liquids, except for the accident of nature that causes one to freeze at temperatures well above the critical temperature of the other. The tendency to form partially miscible liquids asserts itself at high pressures, where the fluids have been compressed to liquid-like densities. The fact that these phase separations often extend to temperatures above the pure component critical points has little to do with the distinctions between gas and liquid phases at low pressures. Fluid-fluid equilibrium would perhaps be a better term than gas-gas equilibrium to describe these high-pressure phase separations. It is interesting to note that these phase separations occur in mixtures of simple molecules, such as helium/hydrogen, helium/methane, and helium/nitrogen where they have been studied at pressures up to 100 kbar, and it has been pointed out that these experiments have important implications for the deep-atmosphere structures of the giant planets (Jupiter, Saturn, Uranus, Neptune) which are composed mainly of light gases (ref. 6,9,15-17).

Fig. 6 shows a system of class III_A in Fig. 2. The gas-liquid critical line has two branches: the one emerging from C_β ends in a critical end point U, where it intersects the three-phase region liquid-liquid-gas, while the second branch, emerging from C_α, passes through both maximum and minimum pressures, merges into a liquid-liquid critical line, and rises to very high pressures at lower temperatures. At temperatures below that of U (e.g., T_1 and T_2) each isotherm includes three distinct two-phase regions: . L_α+G, lying below the three-phase pressure, and L_α+L_β and L_β+G lying above. T_1 has been left unshaded in the interest of clarity. Between the temperatures of C_β and U the L_β+G phase separation forms a closed loop ending in a gas-liquid critical point on the critical line C_βU (e.g., C'_{T2} in Fig. 6[a]). This loop decreases in size with increasing temperature, and vanishes at U. At temperatures above that of U (T_3, T_4 in Fig. 6[a]) a single region of gas-liquid phase separation ends in a critical point. This phase separation vanishes at C_α, and at higher temperatures only a homogeneous single phase exists. At temperatures T_3 and T_4 in Fig. 6 the critical points are unambiguously gas-liquid critical points; however, at T_2 there are two critical points C_{T2} and C'_{T2}. The latter is a gas-liquid critical point, but the former is best described as a liquid-liquid critical point, even though it lies on the same branch of the critical line as the gas-liquid critical points of T_3 and T_4. The upper critical line passes continuously from gas-liquid to liquid-liquid between T3 and T_2, and there is a continuous transition between the gas phase and the

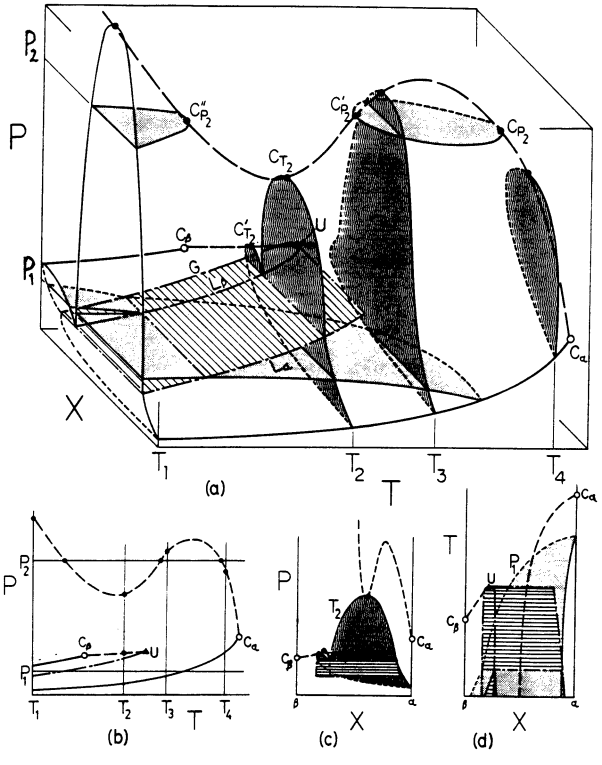

Fig. 6. PTX diagram for a system of class III_A in Fig. 2. The systems carbon dioxide/water and dimethyl ether/water, among others, exhibit this behavior (ref. 19, 20).

β-rich liquid phase in that region. The isobar P_2 in Fig. 6(a) cuts the upper critical line at three critical points, C_{P2}, C'_{P2}, and C''_{P2}. Examples include ethane/methanol (ref. 18), carbon dioxide/water (ref. 19) and dimethyl ether/water (ref. 20). There are many variations in the shapes and locations of the boundary lines in systems of this class, including some in which the three-phase region liquid-liquid-gas lies at pressures above the vapor pressures of both pure components.

Fig. 7 shows a system that has a PT projection of the type shown in Fig. 5(b). Here the three-phase region is shaded by parallel lines, with a portion left unshaded in Fig. 7(a) to show details of isotherm T_2, where it passes through the critical end point U. The three-phase region emerges from the triple point A of the pure component, and ends at high pressures in the boundary UE, where the solid phase E is in equilibrium with gas and liquid phases that become identical at the end point U. Isotherm T_1 lies below the triple point A and consists of a single region of gas-solid phase separation. (It has been left unshaded in Fig. 7 in the interest of clarity.) The isotherm T_2 passes through the end point U, which is a point of tangency between the gas-liquid region (the lower branch of T_2) and the solid-fluid region (the upper branch of T_2). At temperatures between U and

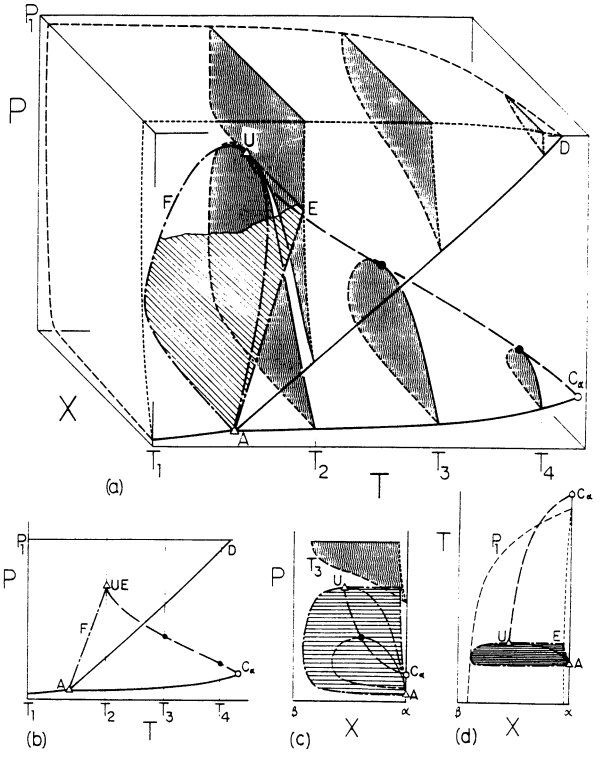

Fig. 7. PTX diagram for a system of class III_{C3} in Fig. 2, with a solid-liquid-gas three-phase region of the type shown in Fig. 5(b). Binary mixtures of neon with argon and methane and of hydrogen with methane, carbon dioxide, ethylene and ethane exhibit this behavior (ref. 21, 22, 25-27).

C_α, increasing pressure increases the mutual solubilities of the gas and liquid phases, which become identical at a point on the critical line $C_\alpha U$. Phase diagrams of the type illustrated by Figs. 5(a) and (b) and Fig. 7 have been carefully studied in a number of systems in which neon or hydrogen is the light component, including mixtures of neon with argon and methane (ref. 21, 22) and mixtures of hydrogen with carbon monoxide, carbon dioxide, methane, ethylene and ethane (ref. 23-27). In the hydrogen/ethylene and hydrogen/ethane systems, the critical end points U lie at pressures of about 6000 bar (ref. 26, 27).

Fig. 8 shows a phase diagram for a system that has a PT projection similar to Fig. 5(d). Here the critical line extending into the diagram from C_α passes through a minimum in temperature (point M) and rises to higher temperatures with increasing pressure. The isotherm T_3 consists of two branches that are tangent at M. As the temperature approaches M from below, the isotherms take on a characteristic "waisted" shape, shown here in isotherm T_2. The systems helium/hydrogen (ref. 6, 8, 9) and helium/nitrogen (ref. 10, 15), among others, exhibit this behavior. The behavior illustrated in Fig. 5(e) is closely related, and has been observed in many helium mixtures, including those with methane, carbon dioxide, ethylene, and others (ref. 5, 28, 29).

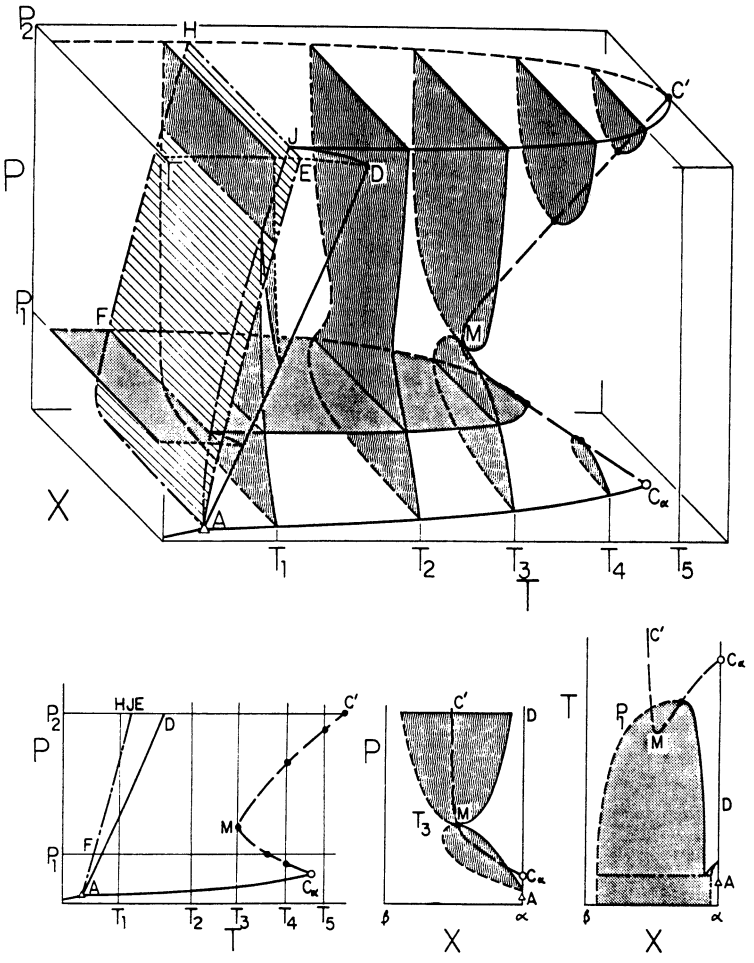

Fig. 8. PTX diagram for a system of class III_{C2} in Fig. 2, with a solid-liquid-gas three-phase region of the type shown in Fig. 5(d). Binary mixtures of helium with hydrogen and nitrogen exhibit this behavior (ref. 6, 8-10, 15,16).

In the hydrogen/helium system the critical line has been observed experimentally at pressures up to 75 kbar and temperatures to 350 K in the remarkable diamond anvil apparatus of Schouten and co-workers (ref. 8, 9, 15). The available evidence suggests that in mixtures of light gases the gas-gas phase separations may persist to much higher temperatures and pressures. It is also well known that the hydrogen/helium system exhibits the so-called barotropic phenomenon--a reversal in the relative densities of two coexisting phases with changes in pressure and/or temperature. If a hydrogen-helium mixture is compressed isothermally at 300 K, for example, a hydrogen-rich solid phase that is less dense than the coexisting helium-rich fluid phase will form at about 65 kbar, and will float to the top of the pressure vessel. In the 1970's Streett and others explored the implications of these phenomena for the deep-atmosphere structure of the planet Jupiter (which is composed mainly of hydrogen and helium) and pointed out that they provide an interesting explanation for, among other things, the "Great Red Spot" that is one of that planet's most dramatic visible features (ref. 30). However, subsequent observations, including those from satellite probes to Jupiter, have shown that the rise of temperature with increasing depth in the Jovian atmosphere is sufficiently rapid that the pressure-temperature trace of the atmosphere is unlikely to cross into the two- and three-phase regions of the hydrogen-helium phase diagram. Nevertheless, in view of the cosmic abundances of hydrogen and helium it is likely that relatively cool bodies composed mostly of these elements exist. If so, the combined effects of phase separations and gravity are among the major factors that influence their interior structures.

Acknowledgements

The author's research on which this review is based has been supported, in part, by grants from the National Science Foundation, the Department of Energy, the Petroleum Research Fund, the Gas Research Institute, Air Products and Chemicals Inc., and the Mobil R&D Corporation.

REFERENCES

1. G. M. Schneider, Adv. Chem. Phys., 17, 1 (1970).
2. G. M. Schneider, Chem. Thermo.l. Vol 2. Specialist Periodical Reports. (Chemical Society, London, Chap. 4, 1978).
3. G. M. Schneider, Angew. Chem. Ind. Ed. Engl., 17, 716 (1978).
4. W. B. Streett and J. L. E. Hill, J. Chem. Phys., 52, 1402 (1970).
5. W. B. Streett, A. L. Erickson and J. L. E. Hill, Phys. Earth & Planet. Interiors, 6, 69 (1972).
6. W. B. Streett, Astrophys. J., 186, 1107 (1973).
7. W. B. Streett, Chemical Engineering at Supercritical Fluid Conditions, p. 3, Ann Arbor Sci. Publishers, Ann Arbor, Michigan (1983), and further references therein.
8. J. A. Schouten, L. C. ven den Bergh and N. J. Trappeniers, Chem. Phys. Lett.,114, 52 (1985).
9. L. C. van den Bergh, J. A. Schouten and N. J. Trappeniers, Physica, 141A, 524 (1987).
10. L. C. van den Bergh and J. A. Schouten, Chem. Phys. Lett., 145, 471 (1988).
11 P. H. Van Konynenberg, PhD Thesis, Univ. of California at Los Angeles (1968).
12. P. H. Van Konynenberg and R. L. Scott, Phil. Trans. Roy., Soc. (London), 298, 495 (1980).
13. J. S. Rowlinson, Liquids and Liquid Mixtures, 2nd Ed., Butterworths, London (1969).
14. W. B. Streett and C. H. Jones, J. Chem. Phys., 42, 398 (1965); and W. B. Streett, Proceedings of the Second International Cryogenics Engineering Conference, Brighton, England, 1968, p. 260, Illife Publ., Guildford, England (1968).
15. W. B. Streett and A. L. Erickson, Phys. Earth & Planet. Interiors, 5 357 (1972).
16. J. A. Schouten and L. C. van den Bergh, Fluid Phase Equilibria, 32, 1 (1986).
17. W. B. Streett, Planetary Atmospheres, p. 363, D. Reidel, Dordrecht, the Netherlands (1971).
18 J. P. Juenen, Phil. Mag., 6, 637 (1903).
19. S. Takenouchi and G. C. Kennedy, Amer. J. Sci., 262, 1055 (1964).
20. M. E. Pozo and W. B. Streett, J. Chem. Eng. Data, 29, 324 (1984).
21. W. B. Streett and J. L. E. Hill, J. Chem. Phys., 54, 5088 (1971).
22. W. B. Streett and J. L. E., Hill, Proc. XIII Int. Congr. Refrig., Vol. 1, Washington, DC (1971).
23. C. Y. Tsang and W. B. Streett, Fluid Phase Equilibria, 6, 261 (1981).
24. C. Y. Tsang and W. B. Streett, Chem. Eng. Sci., 36, 993 (1981).
25. C. Y. Tsang, P. Clancy, J. C. G. Calado and W. B. Streett, Chem. Eng. Commun., 6, 365 (1980).
26. A. Heintz and W. B. Streett, J. Chem. Eng. Data, 27, 465 (1982).
27 A. Heintz and W. B. Streett, Ber. der Bunsenges. Phys. Chem., 87, 298 (1983).
28. D. S. Tsiklis, Dokl. Akad. Nauk. USSR, 86, 1159 (1952).
29. D. S. Tsiklis, Dokl. Akad. Nauk. USSR, 91, 1361 (1953).
30. W. B. Streett, H. I. Ringermacher and G. Veronis, Icarus, 14, 319 (1971).